Available online at www.sciencedirect.com
SCIENCE DIRECT®
Journal of Power Sources 142 (2005) 333–338
JOURNAL OF POWER SOURCES
www.elsevier.com/locate/jpowsour

Short communication

Electrolytic properties of lithium chelatophosphates and application to lithium batteries

Noritoshi Nanbu*, Koji Tsuchiya, Yukio Sasaki*

Department of Nanochemistry, Faculty of Engineering, Tokyo Polytechnic University, 1583 Iiyam Atsugi, Kanagawa 243-0297, Japan

Received 10 September 2003; received in revised form 1 September 2004; accepted 6 September 2004

Abstract

Growing interest has been focused on the development of lithium salts with fluorine atoms and on their application to electric vehicles. We have investigated the electrolytic properties of lithium tris[3-fluoro-1,2-benzenediolato(2-)-*O*,*O*′]phosphate (3-FLTBP) and lithium tris[1,2-benzenediolato(2-)-*O*,*O*′]phosphate (LTBP) and the discharge characteristics of prototype Li/V_2O_5 cells containing ethylene carbonate (EC)-based chain carbonate or EC-based tetrahydrofuran (THF) binary solutions. The introduction of fluorine atoms into a chelatophosphate anion can lead to an increase of conductivity in spite of the enhanced viscosity. Furthermore, we report the coulombic efficiency of the deposition/dissolution cycling for a lithium metal (cycling efficiency of a lithium anode) and the morphology of passivating films formed on a Ni electrode surface in the EC-chain carbonate and the EC–THF binary systems. The addition of a small amount of the 3-FLTBP to EC-based chain carbonate binary solutions containing $LiPF_6$ improves the cycling efficiency. When the cycling efficiency becomes higher, it is found by scanning electron microscope (SEM) that the surface film consists of grains of regular size and that the thickness is relatively thin.

Keywords: Lithium battery; Lithium chelatophosphate; Specific conductivity; Cycling efficiency; Addition effect; Orphology

1. Introduction

There has been a growing demand for the development of novel electrolyte salts for lithium batteries with high energy density and excellent rechargeability. The introduction of fluorine atoms into electrolyte anions can lead to enhanced conductivity and excellent oxidation durability. Lithium salts of chelate compounds are known to be highly thermally stable as compared to common lithium salts. Barthel et al. reported a series of lithium chelatoborates with aromatic rings [1–6], such as lithium bis[3-fluoro-1,2-benzenediolato(2-)-*O*,*O*′]borate. Angell and co-workers synthesized more soluble and electrochemically stable lithium orthoborates based on weakly coordinating anions with aliphatic chelate ligands [7–10], such as lithium bis[1,2-tetra(trifluoromethyl)ethylenediolato(2-)-*O*,*O*′]borate. These chelate compounds can be more stable than the corresponding non-chelated analogs because of the chelate effect. Recently, lithium tetrakis(haloacyloxy)borate, $Li[B(OCORX)_4]$, has been reported [11]. The $Li[B(OCORX)_4]$ is easily soluble in common aprotic solvents and exhibits high conductivity and excellent oxidative durability. However, the $Li[B(OCORX)_4]$ is non-chelated organoborate and thermally unstable.

Sasaki and co-workers at first synthesized three lithium chelatophosphates: lithium tris[1,2-benzenediolato(2-)-*O*,*O*′]phosphate (LTBP) [12], lithium tris[4-methyl-1,2-benzenediolato(2-)-*O*,*O*′]phosphate (4-MLTBP) [13], and lithium tris[3-fluoro-1,2-benzenediolato(2-)-*O*,*O*′]phosphate (3-FLTBP) [14]. They indicated the substituent effect on the thermal and the electrolytic behavior. Recently, Barthel and co-workers also reported three lithium chelatophosphates including the LTBP and the 3-FLTBP [15].

* Corresponding authors. Tel.: +81 46 242 9530; fax: +81 46 242 3000.
E-mail addresses: nanbu@chem.t-kougei.ac.jp (N. Nanbu), sasaki@chem.t-kougei.ac.jp (Y. Sasaki).

0378-7753/$ – see front matter © 2004 Elsevier B.V. All rights reserved.
doi:10.1016/j.jpowsour.2004.09.003

In the present paper, we report the detailed data for the electrolytic properties of 3-FLTBP and LTBP and the discharge characteristics of prototype Li/V_2O_5 cells containing ethylene carbonate (EC)-based chain carbonate or EC-based tetrahydrofuran (THF) binary solutions. Moreover, we have investigated the coulombic efficiency of the deposition/dissolution cycling for a lithium metal (cycling efficiency of a lithium anode) and have studied the morphology of passivating films formed on a Ni electrode surface by scanning electron microscope (SEM), in the EC-chain carbonate and the EC–THF binary systems. The relationship between the cycling efficiency and the morphology is described.

2. Experimental

2.1. Materials

The synthesis and purification of LTBP [12] and 3-FLTBP [14] were previously described. Commercial reagent grade of $LiPF_6$ was used as received. Ethylene carbonate (EC), dimethyl carbonate (DMC), ethylmethyl carbonate (EMC), and diethyl carbonate (DEC) used were battery grade. Commercial tetrahydrofuran (THF) was purified by refluxing overnight with $LiAlH_4$, followed by fractional distillation [16]. The distilled THF was dehydrated by purified molecular sieves (4A) before preparation of the solutions.

2.2. Apparatus and measurements

Specific conductivity of electrolyte solutions was measured by using a conductometer (Toa Electronics, Model CM-60S) with a cell (Model CGT-511B). A prototype Li/V_2O_5 (Toshiba Battery Co. Ltd.) cell (Hohsen Co.) equipped with a glass filter (Advantec Toyo GA-100) as a separator was used in the measurement of discharge curves at a constant current density of 1 mA cm^{-2} (1.84 mA). The energy output based on mass of V_2O_5 (cathode material) was determined from the discharge curves at a cut-off voltage of 2.5 V versus Li|Li^+. Coulombic efficiency of the deposition/dissolution cycling with respect to a lithium metal (cycling efficiency of a lithium anode) was measured with a 6-channel charge/discharge unit (Hokuto Denko, Model HJ-101SM6). A three-electrode cell was used in the measurement of the cycling efficiency. Lithium foil was employed as the auxiliary and the reference electrode. The cycling efficiency was estimated by a galvanostatic plating/stripping method reported by Koch and Brummer [17]. The plating and the stripping current density were 1 mA cm^{-2}. The plated charge density was 300 mC cm^{-2}, and the cut-off voltage was set at −1.0 V versus Li|Li^+ during the anodic stripping process. Direct observation of the morphology of passivating films formed on a Ni electrode surface was carried out with a JEOL JMS-5310 SEM after the 40th cycle.

3. Results and discussion

3.1. Conductivity and viscosity

Conductivity of an electrolyte solution is of practical importance, because it determines the internal resistance and rate performance of the battery. Fig. 1 shows the variations of specific conductivity (κ) of EC-based binary solutions containing 0.5 mol dm^{-3} LTBP or 3-FLTBP with respect to X_{LV} at 25 °C. The symbol X_{LV} denotes a mole fraction of a low-viscosity solvent (THF, DMC, EMC, or DEC). Since the solubility of the chelate compounds in the binary solvents was less than 1 mol dm^{-3}, the concentration of the lithium salt was adjusted to 0.5 mol dm^{-3}. It is well-known that the blending of a high-polarity solvent and a low-viscosity solvent results in the synergistic effect on the conductivity; the conductivity of the electrolyte solution can become higher than that in either one-component solvent system. However, the specific conductivity of the EC–DEC solution containing LTBP decreased with increasing the mole fraction of the DEC, and the mole fraction of the maximum conductivity was not observed. This finding is characteristic of a binary solution in which viscosity of the low-polarity component is very high. The EC was solid at 25 °C, and the EC–DEC mixtures containing the electrolyte salt were solidified under the mole fraction of 0.3 with respect to the DEC.

The conductivity of the binary solutions decreased in the following descending order: EC–THF > EC–DMC > EC–EMC > EC–DEC. This finding can be explained in terms of the viscosity and relative permittivity of the solvent. As a general rule, conductivity of an electrolyte solution is affected by ionic mobility, the charge numbers of ions, the concentration of the electrolyte salt, and the degree of electrolytic dissociation of the salt. The ionic mobility relates to viscosity of the electrolyte solution, while the degree of electrolytic dissociation of the electrolyte salt depends on the permittivity of the medium, ion sizes, and the electronic structures of the

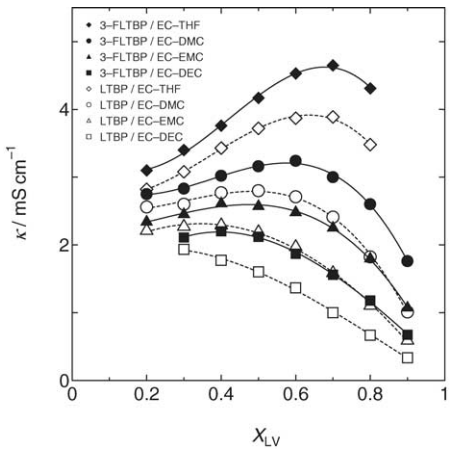

Fig. 1. Specific conductivities (κ) of EC-based binary solutions containing 0.5 mol dm^{-3} LTBP or 3-FLTBP at 25 °C as a function of a mole fraction (X_{LV}) of a low-viscosity solvent (THF, DMC, EMC, or DEC).

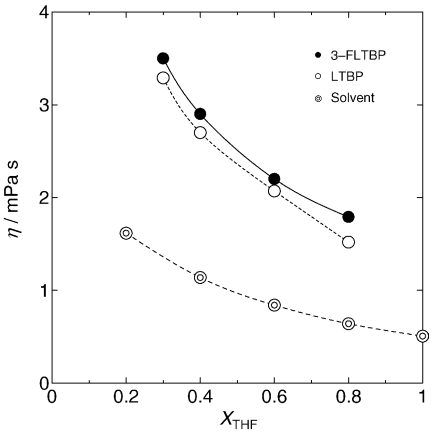

Fig. 2. Viscosity coefficients (η) of EC–THF binary solutions containing 0.5 mol dm^{-3} 3-FLTBP or LTBP at 25 °C as a function of a mole fraction of THF (X_{THF}).

electrolyte salt and the solvents. The values of the viscosity coefficient of THF, DMC, EMC, and DEC at 25 °C are 0.46, 0.59, 0.65, and 0.75 mPa s, respectively. The values of the relative permittivity of THF, DMC, EMC, and DEC at 25 °C are 7.58, 3.12, 2.93, and 2.82, respectively. Therefore, the cooperation between the permittivity and the viscosity leads to a decrease of the conductivity of the electrolyte solution in that order.

As the mole fraction of a low-polarity solvent increases, the viscosity of the solvent mixed with a high-polarity solvent gradually decreases. The viscosity can be regarded as an internal friction. The viscosity of an electrolyte solution increases as compared to that of the solvent, because the electrolyte ions are solvated and the internal friction increases. Fig. 2 shows the variations of viscosity coefficient (η) of EC–THF binary solutions containing 0.5 mol dm^{-3} 3-FLTBP or LTBP with respect to X_{THF} at 25 °C. The viscosity decreased in the sequence 3-FLTBP > LTBP > solvent. A similar relation holds for EC–DMC binary solutions [14]. The viscosity of the solution containing the lithium salt can be governed by the size and mass of the anion. With increasing them, the ionic mobility decreases. On the other hand, the conductivity of the solutions containing 3-FLTBP was higher than that for LTBP, as shown in Fig. 1. A fluorine atom, which has the powerful electron-withdrawing ability, disperses the charge on the anion, and the degree of electrolytic dissociation of the 3-FLTBP is much higher than that for the LTBP [14]. Thus, the concentration of free ions becomes higher in the solution of the 3-FLTBP, and the introduction of fluorine atoms into the LTBP can lead to an increase of conductivity in spite of the enhanced viscosity. In addition, since the anion mobility of the 3-FLTBP is lower than that of the LTBP, the Li^+ conductivity or Li^+ transference number of the 3-FLTBP may become higher. The idea that the charge delocalization in the chelate anion accounts for the higher conductivity also holds for lithium chelatobotates [18–20]. These findings play an important role in the design of novel electrolytes for lithium batteries.

Table 1
Specific energy obtained at a cut-off voltage of 2.5 V vs. Li|Li^+ from discharge curves for EC-based equimolar binary solutions containing 0.5 mol dm^{-3} 3-FLTBP, LTBP, or $LiPF_6$ in Li/V_2O_5 prototype cells at 25 °C. Current density: 1 mA cm^{-2} (1.84 mA)

Electrolyte	Specific energy/Wh kg^{-1}			
	EC–DMC	EC–EMC	EC–DEC	EC–THF
3-FLTBP	300	240	190	350
LTBP	170	130	80	350
$LiPF_6$	430	350	300	430

The conductivities of 3-FLTBP and LTBP were considerably lower than that of $LiPF_6$. For example, the value of the specific conductivity of an EC–DMC (mole ratio 1:1) binary solution containing 0.5 mol dm^{-3} $LiPF_6$ is 9.66 mS cm^{-1}. However, such lower conductivities are improved by mixing with the $LiPF_6$ [14].

3.2. Discharge characteristics of Li/V_2O_5 prototype cells

Fig. 3 shows discharge curves obtained for EC-chain carbonate (DMC, EMC, or DEC) and EC–THF (mole ratio 1:1) binary solutions containing 0.5 mol dm^{-3} lithium salt in Li/V_2O_5 prototype cells at 25 °C. The values of discharge capacity for 3-FLTBP were higher than those for LTBP, but lower than those for $LiPF_6$. Plateau potential regions were narrow on the discharge curves for the lithium chelatophosphates. The energy output per unit mass of V_2O_5 (cathode material) determined from the discharge curves at a cut-off voltage of 2.5 V versus Li|Li^+ is shown in Table 1. The magnitude of the specific energy strongly depends on the smoothness for the insertion of Li^+ into V_2O_5, which can be governed by the conductivity, viscosity and electrochemical stability of the electrolyte solution. The order of the specific energy obtained was essentially same as that of the conductivity in electrolyte solutions: $LiPF_6$ > 3-FLTBP > LTBP with respect to the lithium salt and EC–THF > EC–DMC > EC–EMC > EC–DEC in regard to the EC-based binary solvent.

3.3. Cycling efficiency of lithium anode and morphology of surface films

Coulombic efficiency of the deposition/dissolution cycling with respect to a lithium metal (cycling efficiency of a lithium anode) reflects the reversibility in the processes. Fig. 4 shows the variation of the cycling efficiency of a lithium anode with the cycle number obtained for EC-based binary solutions containing mixtures of $LiPF_6$ and lithium chelatophosphate at 25 °C. It was difficult to measure the cycling efficiency for EC-chain carbonate (DMC, EMC, or DEC) solutions of lithium chelatophosphate, because the efficiency drastically decreased with increasing the cycle number. Thus, mixtures of the lithium chelatophosphate and $LiPF_6$ were used as the electrolyte salts.

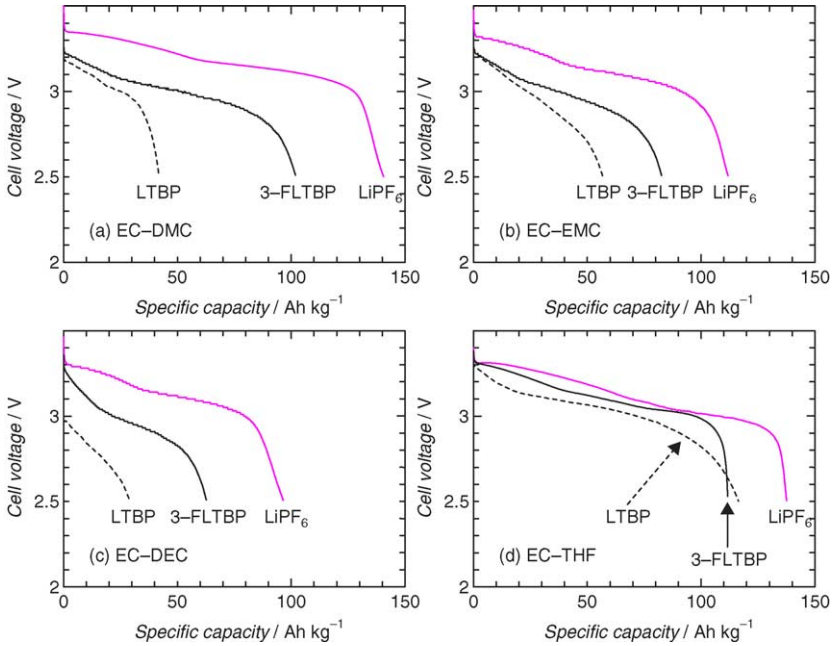

Fig. 3. Discharge curves obtained for (a) EC–DMC, (b) EC–EMC, (c) EC–DEC, and (d) EC–THF (mole ratio 1:1) binary solutions containing 0.5 mol dm^{-3} lithium salt in Li/V_2O_5 prototype cells at 25 °C. Current density: 1 mA cm^{-2} (1.84 mA).

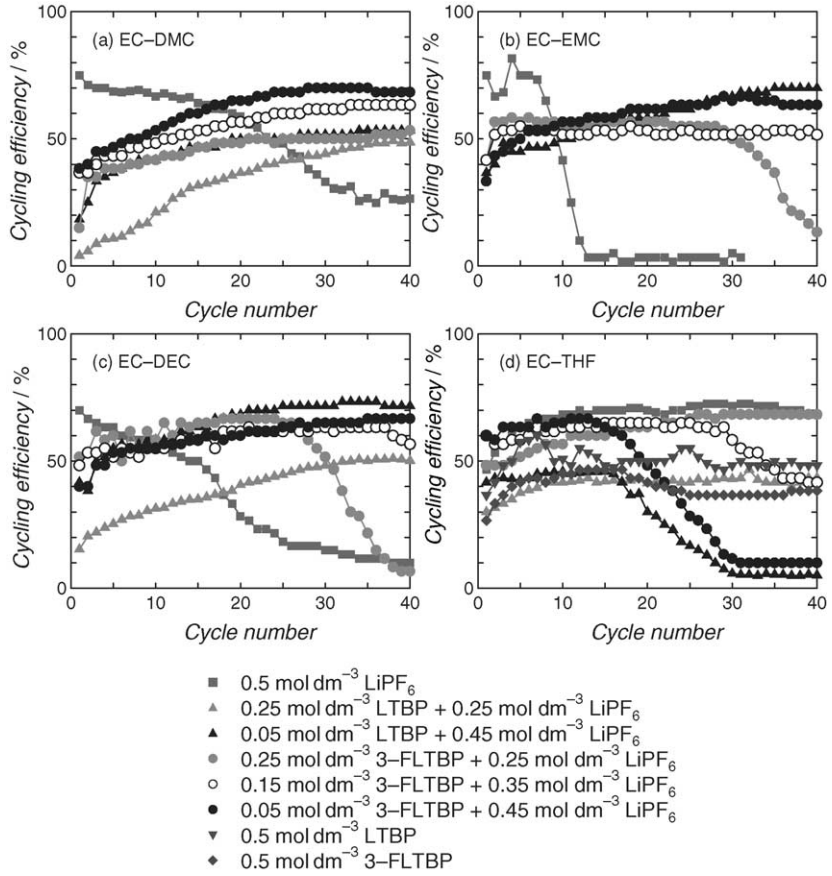

Fig. 4. Variations of cycling efficiency of a lithium anode obtained for (a) EC–DMC, (b) EC–EMC, (c) EC–DEC, and (d) EC–THF (mole ratio 1:1) binary solutions containing mixtures of $LiPF_6$ and lithium chelatophosphate at 25 °C with respect to the cycle number. The plating and the stripping current density were 1 mA cm^{-2}. The plated charge density was 300 mC cm^{-2}, and the cut-off voltage was set at −1.0 V vs. Li|Li$^+$ during the anodic stripping process.

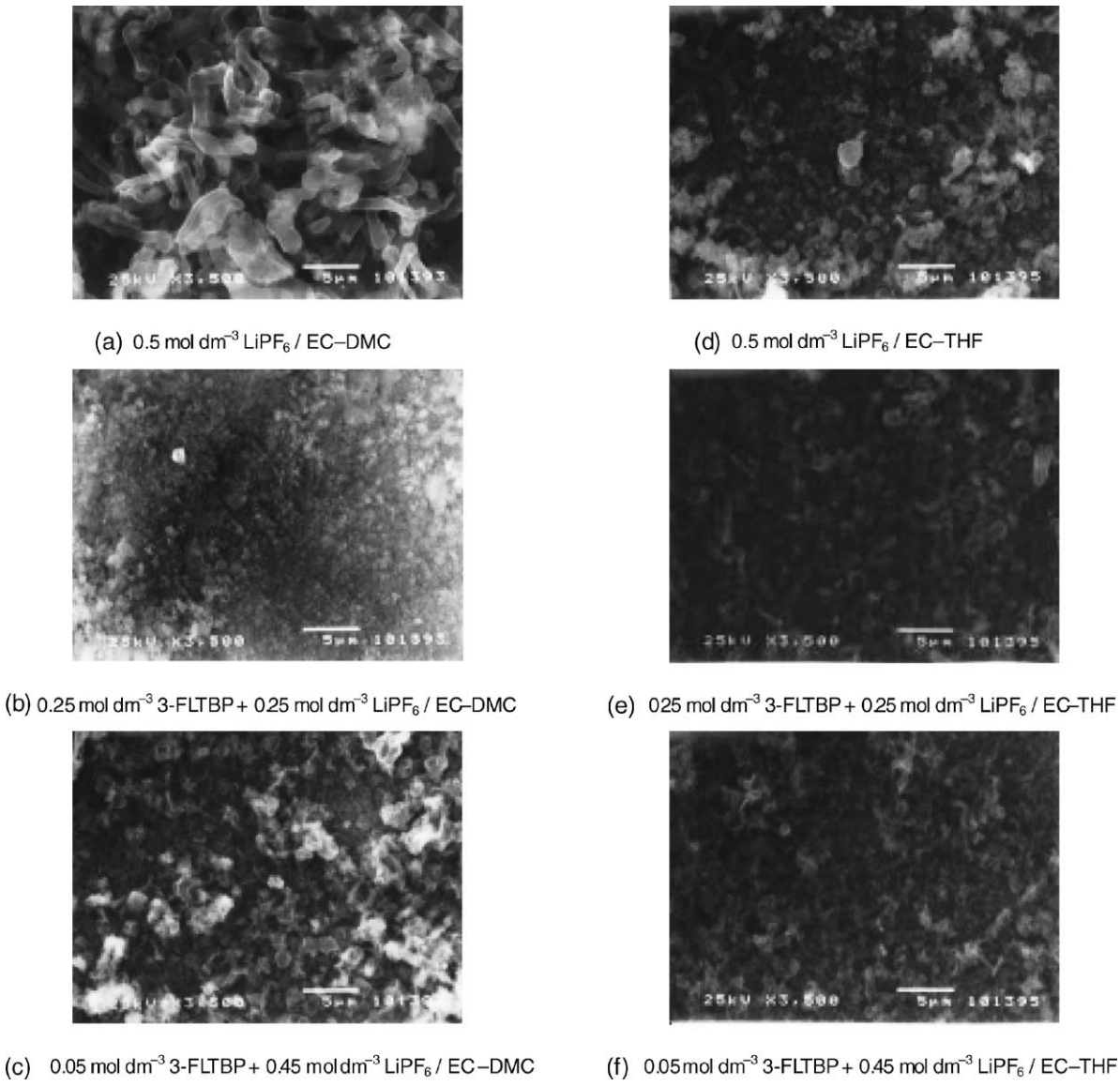

Fig. 5. SEM photographs obtained after the 40th deposition/dissolution cycle of lithium.

The cycling efficiency for EC-chain carbonate (mole ratio 1:1) binary solutions increased with increasing a mole ratio of $LiPF_6$ to 3-FLTBP. The values for equimolar mixtures of $LiPF_6$ and 3-FLTBP were less than 55% beyond the 30th cycle. Moreover, the cycling efficiency for the EC–EMC and the EC–DEC solution decreased rapidly with increasing the cycle number. However, in the case of a 9:1 mole ratio, the values were highly steady and were close to 70% over the range of high cycle numbers. The addition of a small amount of 3-FLTBP can improve the morphology, thickness, density, and chemical composition of a surface film formed by the reaction with lithium deposited on a Ni working electrode and hence can decrease the interfacial resistance between the electrode and the electrolyte solution. Reductive-degradation products of the 3-FLTBP on the lithium anode may form a passive film into which Li^+ ion is permeable. On the other hand, the EC-chain carbonate binary solutions showed the lowest cycling efficiency over the range of high cycle numbers in the absence of the 3-FLTBP. The differences in the cycling efficiency described above were reflected in SEM photographs on a Ni electrode. The SEM photographs shown in Fig. 5 were obtained after the 40th deposition/dissolution cycle of lithium. The morphology of the surface film was homogeneous for the EC−DMC binary solution containing 0.45 mol dm^{-3} $LiPF_6$ + 0.05 mol dm^{-3} 3-FLTBP. The surface film consisted of grains of regular size, and the thickness seemed to be relatively thin. Similar morphology of the surface film was observed for EC−EMC and EC−DEC binary solutions. On the contrary, the morphology of the surface film was coarse and heterogeneous for the EC−DMC binary solution containing 0.5 mol dm^{-3} $LiPF_6$. Particle- and fiber-like deposits were observed. The grain sizes of the surface film

were very small for the EC−DMC binary solution containing an equimolar mixture of $LiPF_6$ and 3-FLTBP. In addition, the surface film seems to be relatively thick.

The cycling efficiency for the EC–DMC binary solution containing 0.45 mol dm^{-3} $LiPF_6$ + 0.05 mol dm^{-3} 3-FLTBP was higher than that in the corresponding binary system of $LiPF_6$ + LTBP over the range of cycle numbers investigated. However, in the case of the EC−DEC binary solution, the value for $LiPF_6$ + 3-FLTBP was slightly lower after the 15th cycle. The introduction of fluorine atoms into the LTBP may change the chemical composition of the surface film, and the difference can be reflected in the cycling efficiency.

The cycling efficiency for an EC–THF (mole ratio 1:1) binary solution containing an equimolar mixture of 3-FLTBP and $LiPF_6$ was highly steady and ca. 70% over the range of high cycle numbers. This value was comparable to that in a one-component system of $LiPF_6$. The cycling efficiency decreased when a mole ratio of $LiPF_6$ to 3-FLTBP increased or decreased. The SEM photographs for the equimolar binary mixture of $LiPF_6$ and 3-FLTBP showed that surface film was uniform in grain sizes. On the other hand, in the case of a 9:1 mole ratio, the morphology of the film was relatively coarse and heterogeneous.

The cycling efficiency strongly depends on the morphology, thickness, density, and chemical composition of the surface film and is not always influenced by the bulk properties of the electrolyte solution such as conductivity and viscosity [21]. For example, the value of specific conductivity in an EC–DMC (mole ratio 1:1) binary solution containing 0.5 mol dm^{-3} $LiPF_6$ is 9.66 mS cm^{-1}, while the value for an EC–DMC binary solution containing 0.5 mol dm^{-3} equimolar binary mixture of 3-FLTBP and $LiPF_6$ is 5.73 mS cm^{-1}. The cycling efficiency was as low as 23% after the 40th cycle in the one-component system of $LiPF_6$, whereas that was 53% in the binary system of 3-FLTBP and $LiPF_6$. The chemical composition of the surface film formed due to reduction of electrolytes in the binary system can also be different from that in the one-component system. A proper amount of fluorine in the surface film may be desirable for the permeation of Li^+ ions.

The oxidative decomposition of the lithium chelatophosphates proceeds in a potential range of 3.6–4.1 V versus $Li|Li^+$ [14]. Therefore, the use of the lithium chelatophosphates as additives may be effective for preventing overcharge on the V_2O_5 cathode as well as for forming a better protection film on the Li anode.

4. Conclusions

We have reported the detailed data for the electrolytic properties of 3-FLTBP and LTBP and the application to lithium batteries. The solutions containing the 3-FLTBP showed higher conductivity than that for the LTBP in spite of the enhanced viscosity. This is because the degree of electrolytic dissociation of the 3-FLTBP is higher. The values of discharge capacity obtained for the 3-FLTBP in prototype Li/V_2O_5 cells were higher than those for the LTBP, but lower than those for $LiPF_6$. The addition of a small amount of the 3-FLTBP to EC-based chain carbonate binary solutions containing $LiPF_6$ improved the cycling efficiency of a lithium anode and the morphology of passivating films formed on a Ni electrode surface. When the cycling efficiency became higher, the SEM photograph obtained after the 40th cycle showed that the surface film was uniform in grain sizes and that the thickness was relatively thin.

References

[1] J. Barthel, M. Wühr, R. Buestrich, H.J. Gores, J. Electrochem. Soc. 142 (1995) 2527.
[2] J. Barthel, R. Buestrich, E. Carl, H.J. Gores, J. Electrochem. Soc. 143 (1996) 3565.
[3] J. Barthel, R. Buestrich, E. Carl, H.J. Gores, J. Electrochem. Soc. 143 (1996) 3572.
[4] J. Barthel, R. Buestrich, H.J. Gores, M. Schmidt, M. Wühr, J. Electrochem. Soc. 144 (1997) 3866.
[5] J. Barthel, M. Schmidt, H.J. Gores, J. Electrochem. Soc. 145 (1998) 17.
[6] J. Barthel, A. Schmid, H.J. Gores, J. Electrochem. Soc. 147 (2000) 21.
[7] W. Xu, C.A. Angell, Electrochem. Solid-State Lett. 3 (2000) 366.
[8] W. Xu, C.A. Angell, Electrochem. Solid-State Lett. 4 (2001) 1.
[9] K. Xu, S. Zhang, T.R. Jow, W. Xu, C.A. Angell, Electrochem. Solid-State Lett. 5 (2002) 26.
[10] W. Xu, A.J. Shusterman, M. Videa, V. Velikov, R. Marzke, C.A. Angell, J. Electrochem. Soc. 150 (2003) 74.
[11] H. Yamaguchi, H. Takahashi, M. Kato, J. Arai, J. Electrochem. Soc. 150 (2003) 312.
[12] M. Handa, M. Suzuki, J. Suzuki, H. Kanematsu, Y. Sasaki, Electrochem. Solid-State Lett. 2 (1999) 60.
[13] N. Nanbu, T. Shibazaki, Y. Sasaki, Chem. Lett. (2001) 862.
[14] N. Nanbu, K. Tsuchiya, T. Shibazaki, Y. Sasaki, Electrochem. Solid-State Lett. 5 (2002) 202.
[15] M. Eberwein, A. Schmid, M. Schmidt, M. Zable, T. Burgemeister, J. Barthel, W. Kunz, H.J. Gores, J. Electrochem. Soc. 150 (2003) 994.
[16] J.A. Riddick, W.B. Bunger, T.K. Sakano, Organic Solvents, 4th ed., Wiley, New York, 1986.
[17] V.R. Koch, S.B. Brummer, Electrochim. Acta 23 (1978) 55.
[18] Y. Sasaki, M. Handa, K. Kurashima, T. Tonuma, K. Usami, J. Electrochem. Soc. 148 (2001) 999.
[19] Y. Sasaki, N. Nanbu, in: N. Kumagai, S. Komaba (Eds.), Materials Chemistry in Lithium Batteries, Research Signpost, 2002, p. 415.
[20] N. Nanbu, T. Shibazaki, Y. Sasaki, Electrochemistry 71 (2003) 1205.
[21] Y. Sasaki, M. Handa, S. Sekiya, K. Kurashima, K. Usami, J. Power Sources 97/98 (2001) 561.